

ALFVÉN WAVE EXPERIMENTS WITH LIQUID RUBIDIUM IN A PULSED MAGNETIC FIELD

*Th. Gundrum¹, J. Forbriger¹, Th. Herrmannsdörfer¹,
G. Mamatsashvili¹, S. Schnauck^{1,2}, F. Stefani¹, J. Wosnitza¹*

¹ *Helmholtz-Zentrum Dresden – Rossendorf, Bautzner Landstr. 400, 01328 Dresden, Germany*

² *Anton Pannekoek Institute for Astronomy, University of Amsterdam, Postbus 94249, 1090 GE Amsterdam, The Netherlands*

Abstract: Magnetic fields are key ingredients for heating the solar corona to temperatures of several million Kelvin. A particularly important region with respect to this is the so-called magnetic canopy below the corona, where sound and Alfvén waves have roughly the same speed and can, therefore, easily transform into each other. We present the results of an Alfvén-wave experiment with liquid rubidium carried out in a pulsed field of up to 63 T. At the critical point of 54 T, where the speeds of Alfvén waves and sound coincide, a new 4 kHz signal appears in addition to the externally excited 8 kHz torsional wave. This emergence of an Alfvén wave with a doubled period is in agreement with the theoretical predictions of a parametric resonance between the two wave types. We also present preliminary results from numerical simulations of Alfvén and magneto-sonic waves using a compressible MHD code.

1. Introduction Shortly after their theoretical prediction in 1942 [1], the existence of Alfvén waves was confirmed in liquid-metal experiments by Lundquist [2] and Lehnert [3]. Later, they were studied in much detail in large-scale plasma experiments, a comprehensive summary of which can be found in the paper by Gekelman [4]. Nowadays, Alfvén waves are known to play a key role in many phenomena in astrophysical and fusion-related plasmas [5]. They are, in particular, one of the main candidates to explain the heating of the solar corona [6, 7, 8] to temperatures of several million Kelvin. A particularly important region in this matter is the so-called magnetic canopy below the corona (see Fig. 1), where sound and Alfvén waves have roughly the same speed and can, therefore, easily transform into each other [9]. However, this “magic point” has remained inaccessible to experiments until recently: while in plasma experiments the Alfvén speed is typically much higher than the speed of sound, in all previous liquid-metal experiments it has been significantly lower.

Recent developments in reaching pulsed magnetic fields above 50 Tesla have revealed new prospects for Alfvén-wave experiments with liquid metals. The main idea of our experiment [10] was, therefore, to utilize high pulsed magnetic fields to allow Alfvén waves whose propagation speed increases proportionally to the magnetic field to cross the sound speed of $c_s = 1260$ m/s at the “magic point” of 54 T, when using liquid rubidium. By injecting an alternating current at the bottom of the rubidium container and exposing it to the pulsed magnetic field of up to 63 T (Fig. 2), it became possible to generate Alfvén waves in the melt,

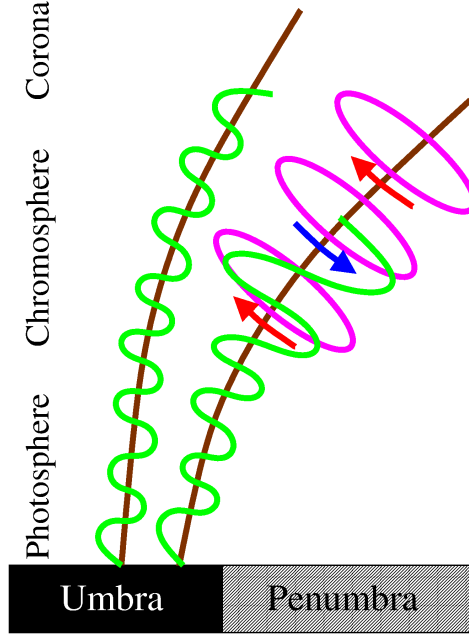


Figure 1: Illustration of the transformation of magneto-sonic waves (green) into period-doubled torsional Alfvén waves (purple) in the solar chromosphere where $v_a \approx c_s$ (after [7]). Such torsional waves, travelling along magnetic field lines (brown), have recently been measured in the solar chromosphere [8].

whose upward motion was measured at the expected speed, similarly to previous experiments [13]. In that paper, we described that, while all measurements up to the “magic point” of 54 T were dominated by the 8 kHz signal of the injected AC current, exactly at this point a new 4 kHz signal appeared. This sudden emergence of period doubling was in perfect agreement with the theoretical predictions of a parametric resonance as described by Zaqarashvili and Roberts [9]. According to their theory, the Alfvén wave drives the sound wave through the ponderomotive force, while the sound wave returns energy back to the Alfvén wave through swing excitation. Here, we summarize the main experimental outcomes of [10], and complement them with first numerical results on the interaction of Alfvén- and magneto-sonic waves that were obtained with the compressible MHD-code PLUTO [11].

2. The experiment The experiments were carried out within a long-pulse coil [12] of the Dresden High Magnetic Field Laboratory (HLD) at Helmholtz-Zentrum Dresden-Rossendorf (HZDR). Situated in its central bore of 24 mm diameter, the (warm) liquid rubidium experiment was shielded thermally from the liquid-nitrogen cooled copper coil by a Dewar wall. The rubidium-filled stainless steel container (Fig. 2a), with inner diameter 10 mm and 60 mm height, was embedded into a holder for the pick-up and compensation coils (Fig. 2b). During the experiment, a controlled current source (Agilent 33220A and Rohrer PFL-2250-28-UDC415-DC375) delivered a very stable sinusoidal cw current with constant amplitude of 5 A and frequency of 8 kHz, which was applied between the lower contact (LC) and the three contacts (RC) encircling the lower rim of the container (Fig. 2c). The resulting current density j_r , which is concentrated in the bottom

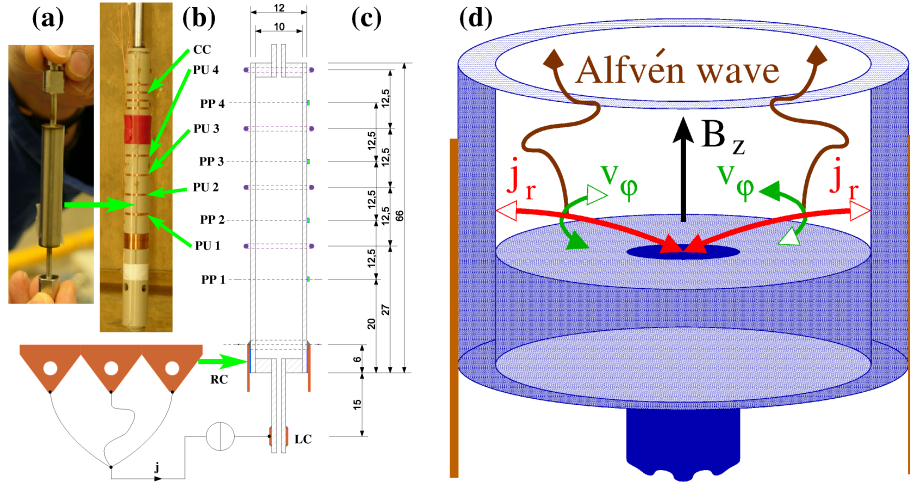


Figure 2: Experimental setting. (a) Stainless-steel container filled with liquid rubidium. (b) Holder with four pickup coils (PU 1-4) and four compensation coils (CC). (c) Geometrical details of the construction. PP 1-4 denote four electric-potential probes soldered on the container. The three orange triangles indicate the rim contacts (RCs) encircling the bottom part of the container. LC is the lower contact. (d) Schematic for the driving of the torsional Alfvén wave in the lower part of the container. After [10].

layer of the rubidium and basically directed in radial direction, together with the strong vertical field B_z , generates an azimuthal Lorentz force density $f_\phi = j_r \times B_z$ that drives a torsional Alfvén wave in the fluid, as illustrated in Fig. 2d. This upward propagating wave can be followed by the four stacked electric-potential probes PP 1-4, which measure the electromotive force (emf) $U = v_\phi B_z r$ induced by the azimuthal velocity component v_ϕ . As was shown in the supplemental material of [10], the correlation between the signals of those voltage probes allows us to identify the Alfvén speed which depends on the instantaneous magnetic field $B_z(t)$ according to $v_a(t) = B_z(t)/(\mu_0 \rho)^{1/2}$.

The four pick-up coils PU 1-4, in turn, measure the induction by the time-dependent azimuthal current j_ϕ , which results from the interaction of radial velocity components v_r with B_z . The voltages measured at the pick-up coils are, though in a non-trivial manner, representative of the sound wave in the liquid rubidium. As shown in [10], their spectrum contains a strong 16 kHz component, arising from the ponderomotive force, but also an 8 kHz signal of comparable amplitude, an effect that has also been detected in a previous experiment by Iwai [14].

A first result of our numerical simulations of the nonlinear coupling between the externally forced Alfvén waves and the magneto-sonic with doubled frequency and vertical wavenumber is shown in Fig. 3. The simulation was done with the compressible, finite-volume Godunov-type code PLUTO [11]. The torsional Alfvén waves are continually driven by an external toroidal force, which is concentrated near the bottom of the cylinder and oscillates with a fixed frequency of 8 kHz, mimicking the Lorentz force in the experiment. The structure of resulting Alfvén

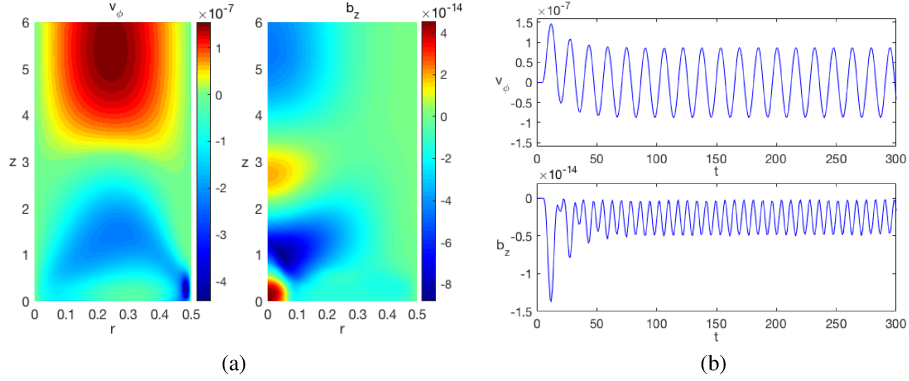


Figure 3: Numerical simulations of the Alfvén-wave experiment at a Lundquist number of 45, corresponding to a magnetic field amplitude of $B_0 = 35$ T in the experiment. (a) Snapshots of the toroidal velocity v_ϕ corresponding to the Alfvén wave driven by the external forcing, and the perturbation b_z of the vertical magnetic field corresponding to the generated magneto-sonic waves in the (r, z) -plane. (b) Time-development of these quantities at the fixed point $(r_0, z_0) = (0.25, 2.24)$ (in units of the cylinder diameter $d = 10$ mm) in the container (time in units of d/c_s). Note that the frequency and wavenumber of the magneto-sonic waves are about twice larger than those of the Alfvén waves.

waves consist of a large-scale standing wave with dominant toroidal velocity v_ϕ and magnetic field perturbations b_ϕ , which vary in time with the same frequency as the forcing. Their vertical wavelength, determined by the Alfvén wave dispersion relation for this frequency, approximately fits into the container height (Fig. 3a, left panel). The magneto-sonic waves excited by the Alfvén waves have in turn a dominant vertical velocity, v_z , and magnetic field perturbations b_z . Their structure is shown in Fig. 3a, right panel, which consists of a standing wave with about twice shorter wavelength and doubled oscillating frequency (see Fig. 3b).

3. Main results Figure 4 summarizes the main results of one experimental run, carried out with a temperature of 50°C at which rubidium is liquid. The experiment starts by charging the capacitor bank of HLD up to a voltage of 22 kV. After releasing (at $t = 20$ ms in Fig. 4a) the stored energy, the axial magnetic field increases quickly to attain a maximum value of 63.3 T at $t = 53$ ms. Afterwards, the field decays slowly, reaching a value of 2.1 T at the end of the interval shown here ($t = 150$ ms). The period during which the field exceeds the critical value of 54 T extends from 40.5 to 66 ms, as indicated by the dashed red lines (see Fig. 4a).

The voltage $U_{\text{LC-RC}}$ measured between the contacts LC and RC comprises three contributions: First, the usual Ohmic voltage drop over the contacts (with an amplitude of approximately 5 mV, as observed at the start and end of the magnetic-field pulse when the magnetic field is close to zero); second, a certain long-term trend resulting from the time derivative of the pulsed field; third, a significant electromotive force (EMF) $v_\phi \times B_z$ arising from the interaction of the toroidal velocity v_ϕ of the generated torsional Alfvén wave with the axial magnetic field B_z .

Even without having a detailed numerical analysis at hand yet, we can plausibilize the measured oscillation amplitude of this EMF: with an applied current

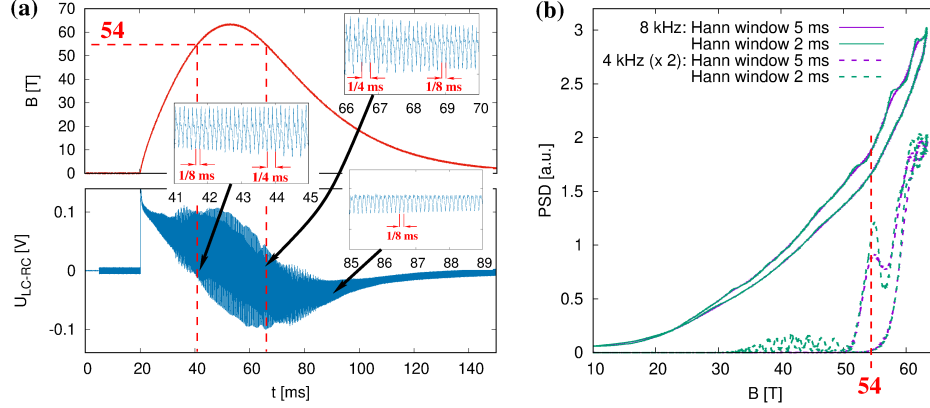


Figure 4: (a) Time dependence of the pulsed magnetic field and of the voltage measured at the lower contact. The red dashed lines indicate the instants where the critical field strength of 54 T is crossed. The insets of (a) detail one normal region in the falling branch (between 85 and 89 ms) with a mainly pure 8 kHz signal, and the two transition regions, where the double-period signal due to torsional Alfvén wave starts and ceases to exist. (b) Power spectral density (PSD) of the 8 and 4 kHz coefficients of the voltage U_{LC-RC} from Figs. 4(a) and for two different von Hann windows. While the 8 kHz signal shows a very monotonic (quadratic) increase with the field, the 4 kHz signal appears only above the “magic point” of 54 T. The peak at this very value, corresponding to the falling branch, confirms the theoretic prediction of [9]. The increase of the signal beyond this field value is not yet fully understood. See [10].

amplitude of 5 A, and taking into account the contact geometry, we obtain a current density of about $j_r \approx 100 \text{ kA/m}^2$, leading (with an axial field $B_z = 50 \text{ T}$ and a density of $\rho = 1490 \text{ kg/m}^3$) to an azimuthal acceleration of $a_\varphi \approx 3000 \text{ m/s}^2$. Assumed to act over half an excitation period (i.e., $1/16 \text{ ms}$), this acceleration would generate flow velocities of $v_\varphi \approx 20 \text{ cm/s}$, which, when integrated over the container’s radius of $r = 5 \text{ mm}$, induce a voltage of $v_\varphi B_z r \approx 50 \text{ mV}$. Encouragingly, this very rough estimate is in good agreement with the measured amplitude of the voltage oscillation as seen in the high-field segment of Fig. 4a. In light of the high quality of the Alfvén-wave resonator (as indicated by a Lundquist number of 67) this agreement is not that surprising. The three insets of Fig. 4a show in more detail one “normal” segment within the falling branch of the pulsed field (between 85 and 89 ms), characterized by a more or less pure 8 kHz signal, and the two transition periods in the vicinity of 54 T, where the double-period 4 kHz signal due to a secondary torsional Alfvén wave starts and ceases to exist.

The measured voltage U_{LC-RC} is now analyzed in detail by means of a windowed Fourier transform (or Gabor transform), from which we can infer the instantaneous Power Spectral Density (PSD) for different frequencies, including both the rising and falling branches of the pulsed magnetic field. As shown in [10], the dominant feature of this spectrogram is, unsurprisingly, the 8 kHz signal. More interesting, however, is the emergence of a new signal at 4 kHz at the threshold of 54 T where $v_a = c_s$. Figure 4(b) confirms the nearly quadratic dependence of the PSD of the externally driven 8 kHz mode (with only a slight difference between the rising and the falling branch), which one expects from the linear dependence of the torsional velocity on B_z . We also observe a clear peak of the 4 kHz signal

close to 54 T, coming from the falling branch, and another peak behind, coming from the rising branch. Actually, this persistence of the 4 kHz signal for $v_a > c_s$ is not explained using the parametric resonance model of [9] without difficulty and, therefore, needs a more detailed analysis.

4. Conclusions In this paper, we have summarized the Alfvén-wave experiments with liquid rubidium carried out at the HLD of HZDR which have, for the first time, allowed us to cross the threshold $v_a = c_s$ where the transformation between magneto-sonic and Alfvén waves becomes particularly efficient. Indeed, at that point we have observed a secondary torsional wave with doubled period, in good agreement with the theoretical prediction of swing-excitation between magneto-sonic and Alfvén waves. In a next step, we will try to support the experimental work with more detailed numerical simulations using the PLUTO code. This will help us to better understand the observed effects, and also to optimize the parameters of follow-up experiments.

Acknowledgments We acknowledge support of the HLD at HZDR, a member of EMFL, and the DFG through the Würzburg-Dresden Cluster of Excellence on Complexity and Topology in Quantum Matter-ct.qmat (EXC 2147, Project No. 390858490). F. S. acknowledges further support by the European Research Council (ERC) under the European Union’s Horizon 2020 Research and Innovation Programme (Grant No. 787544). We thank Jürgen Hüller for his assistance in the adventurous filling procedure of the rubidium container, and Frank Arnold, Larysa Zviagina, Carsten Putzke, Karsten Schulz, and Marc Uhlarz for their help in preparing and carrying out the experiment.

REFERENCES

1. H. ALFVÉN Existence of electromagnetic-hydrodynamic waves. *Nature* , vol. 150 (1942), p. 405.
2. S. LUNDQUIST Experimental demonstration of magneto-hydrodynamic waves. *Nature* , vol. 164 (1949), p. 149.
3. B. LEHNERT Magneto-hydrodynamic waves in liquid sodium. *Phys. Rev.* , vol. 94 (1954), p. 815.
4. W. GEKELMAN Review of laboratory experiments on Alfvén waves and their relationship to space observations. *J. Geophys. Res.* , vol. 104 (1999), p. 14417.
5. N.F. CRAMER The physics of Alfvén waves. *The physics of Alfvén waves*. (Wiley, Berlin, 2005)
6. S. TOMCZYK, S.M. MCINTOSH, S.L. KEIL, P.G. JUDGE, T. SCHAD, T.H. SHEELEY, J. EDMONDSON Alfvén waves in the solar corona. *Science* , vol. 317 (2007), p. 1192.
7. S.D.T. GRANT ET AL. Alfvén wave dissipation in the solar chromosphere. *Nature Phys.* , vol. 14 (2018), p. 480.
8. A.K. SRIVASTAVA ET AL. High-frequency torsional Alfvén waves as an energy source for coronal heating. *Sci. Rep.*, vol. 7 (2017), p. 43147.
9. T.V. ZAQARASHVILI, B. ROBERTS Two-wave interaction in ideal magnetohydrodynamics. *Astron. Astrophys.*, vol. 452 (2006), p. 1053.
10. F. STEFANI, J. FORBRIGER, T. GUNDRUM, T. HERRMANNSDÖRFER, J. WOSNITZA Mode conversion and period doubling in a liquid Rubidium Alfvén-wave experiment with coinciding sound and Alfvén speeds. *Phys. Rev. Lett.*, vol. 127 (2021), Art. No. 275001.
11. A. MIGNONE ET AL. PLUTO: A Numerical Code for Computational Astrophysics. *Astrophys. J. Suppl.*, vol. 170 (2007), p. 228. <http://plutocode.ph.unito.it/> .

12. J. WOSNITZA ET AL. Dresden pulsed magnetic field facility. *J. Magn. Magn. Mat.*, vol. 310 (2007), p. 2728.
13. T. ALBOUSSIÈRE ET AL. Experimental evidence of Alfvén wave propagation in a Gallium alloy. *Phys. Fluids*, vol. 23 (2011), Art. No. 096601.
14. K. IWAI, K. SHINYA, K. TAKASHI, R. MOREAU Pressure change accompanying Alfvén waves in a liquid metal. *Magnetohydrodynamics*, vol. 39 (2003), p. 245.